Slit Map : Conformal Parameterization for Multiply Connected Surfaces

Xiaotian Yin[1], Junfei Dai[2], Shing-Tung Yau[3], and Xianfeng Gu[1]

[1] Center for Visual Computing
State University of New York at Stony Brook
[2] Center of Mathematics Science
Zhejiang University
[3] Mathematics Department
Harvard University

Abstract. Surface parameterization is a fundamental tool in geometric modeling and processing. Most existing methods deal with simply connected disks. This work introduces a novel method to handle multiply connected surfaces based on holomorphic one-forms. The method maps genus zero surfaces with arbitrary number of boundaries to an annulus with concentric circular slits. Any two boundaries can be chosen to map to the inner circle and the outer circle, the other boundaries to slits. Equivalently, the surfaces can be mapped to a rectangle with horizontal slits.
Compared to existing linear methods that require surface partition, this method is more intrinsic and automatic. Compared to the existing holomorphic one-form method that requires double covering, it is more efficient and has better control over singularities. Compared to the existing Ricci flow method, this one is linear and simpler.
The proposed method has many merits. The images of boundaries are parallel line segments. This regularity not only helps improve the accuracy for surface matching with boundaries, but also makes quad-remeshing or mesh-spline conversion conversion convenient. The whole rectangle in texture domain is fully occupied without any gap or overlapping; this improves the packing efficiency for texture mapping. The positions of the slits are completely determined by the surface geometry, which can be treated as the finger print of the surface to classify surfaces by conformal equivalence.
The algorithm is thoroughly explained in detail. Experimental results are demonstrated to show the usefulness of the algorithm for multiply connected domains.

Key words: conformal parameterization, slits, holomorphic one-form

1 Introduction

Surface conformal parameterization is a fundamental tool in geometric modeling and processing. It is an essential technique for many applications, such as texture

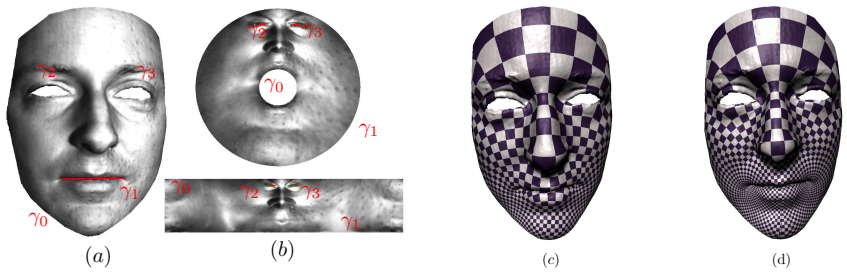

Fig. 1. Slit map. (a) shows the original surface, which is a multiply connected domain; (b) shows the slit domains. The top is the circular slit domain with outer circle γ_1 and inner circle γ_0; the bottom is the parallel slit domain with upper side γ_0 and lower side γ_1. (c) shows the conformal texture mapping by the circular slit map. (d) shows the conformal texture mapping by the parallel slit map.

mapping, surface matching, registration and tracking, re-meshing, mesh-spline conversion and so on.

Most existing parameterization methods focus on *simply connected surfaces*, namely genus zero surfaces with a single boundary. According to Reimann's mapping theorem, any simply connected surface can be conformally mapped to the unit disk, as shown in figure 2. The mapping is not unique. Two conformal mappings differ by a Möbius transformation of the unit disk.

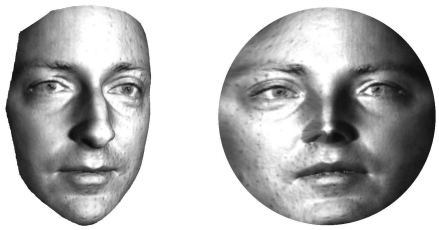

Fig. 2. Riemann mapping for a simply connected surface.

In practice, surfaces are usually with complicated topologies. In order to parameterize them using conventional methods, surfaces need to be partitioned to simply connected disks first. This will introduce many artificial cuts and destroy the intrinsic geometric properties of the original surfaces. In many geometric modeling and processing applications, such as mesh-spline conversion and shape classification, it is highly desirable to compute the parameterization without partitioning. Our work focuses on the global parameterization of a broad class of surfaces.

A *multiply connected surface* is a genus zero surface with multiple boundaries, as shown in figure 1. Similar to the Riemann mapping theory, any multiply

connected surface can be conformally mapped to some canonical domains. One of such domains is the *circular slit domain*, which is an annulus with concentric arc slits, as shown at the top of figure 1b; The other is the *periodic parallel slit domain*, which is a strip with parallel slits, as shown at the bottom of figure 1b. Two boundaries of the surface are mapped to the inner and outer boundaries of the circular slit domain, and all the other boundaries are mapped to the circular slits.

Compared to the simply connected case, the conformal mapping of multiply connected surfaces is much more complicated. Two surfaces are *conformally equivalent*, if there exists a conformal map between them. We can pick a canonical representative for each conformal equivalence class. For example, all simply connected surfaces are conformally equivalent, and the unit disk can serve as the sole canonical representative. But multiply connected surfaces are in general not conformally equivalent. For each conformal equivalence class of such surfaces we need a separate circular slit domain as the canonical representative. In this sense, the conformal parameterization algorithm for multiply connected surfaces must compute both the mapping and the target domain; whereas the algorithm for simply connected surfaces only needs to compute the mapping, since the domain could be unique.

1.1 Contributions

In this paper we propose a novel method of conformal parameterization for multiply connected surfaces. It maps the surface to circular slit domain or parallel slit domain conformally. The algorithm is based on finding certain holomorphic one-forms whose integration along boundaries satisfies special constraints. To the best of our knowledge, this is the first work to directly handle multiply connected surfaces by a linear method.

Slit mapping has many merits for geometric modeling and processing tasks.

First, slit mapping maps the whole surface to a rectangle, with all the boundaries mapped to parallel slits. This regularity not only helps improve the accuracy for surface matching with boundaries, but also makes quad-remeshing, mesh-spline conversion convenient.

Second, the whole rectangle in the parallel slit domain is fully occupied without any gap or overlapping, which improves the packing efficiency of texture mapping.

Third, the positions of the slits in the regular domain are completely determined by the surface geometry, which can be treated as the finger print to classify surfaces by conformal equivalence.

Fourth, the whole pipeline is based on manipulation of one-forms, which is a linear process that is very efficient and stable. Plus, the whole pipeline is very easy to implement.

1.2 Related Work

In recent years, many excellent algorithms have been developed in surface parameterization. In this work, we only briefly review the most related works. For more thorough references on parameterization methods, we refer readers to the the following excellent surveys: [4] by Floater et al and [2] by Sheffer et al.

Many existing methods target at simply connected surfaces, either with fixed boundary condition ([3], [5] and etc) or free boundary condition [[6], [7], [1], [8] and etc]. These methods can not be applied to the multiply connected surfaces directly, because they can not guarantee the mapping to be diffeomorphism.

A common way to generalize the parameterization methods for simply connected surfaces is by "cutting-and-packing". This approach has been adapted by Cohen-Steiner et al. [9], Garland et al. [10], Maillot et al. [11] and Sander et al. [12]. All these methods require to cut the surface into multiple patches, parameterize them separately and then pack them together in the texture domain. Because the partitioning process is artificial, global geometric properties of the surfaces will be lost. Furthermore, the conformality can not be achieved along the patch boundaries.

Global method without segmentation is proposed by Gu et al. [13][14]. They used holomorphic one-forms as the underlying tool. But for multi-hole annuli, this method needs double covering to make the surface close, which will increase the computational cost. Our slit method, on the other hand, does not require double covering and is more efficient. Furthermore, their method can not control the positions of singularities in the parameterization. Our method has full control of the singularities. The method in [14] is general for surfaces with arbitrary topologies. In our work, we focus on multiply connected surfaces, therefore the algorithm is simplified to skip the computing of homology basis.

One-form has also been used for vector fields decomposition and smoothing [23]. Discrete one-forms on meshes were studied in [18]. Tong et al. [20] used harmonic one-forms for surface parameterization. They enlarge the space of harmonic one-forms by allowing additional singular points on the surface. Kälberer et al. applied one-forms for surface parameterization combining with branch covering in [21], where the parameter lines are governed by a given frame field. In [22] Fisher et al. used one-forms for designing tangent vector fields on surfaces with complicated topologies.

Another method for multiply connected surfaces is discrete Ricci flow, proposed by Jin et al. [15]. They can prescribe the target curvature of boundaries, so that the target domain has regular shape, such as a unit disk with multiple inner circle boundaries. But it requires non-linear optimization. In our method only linear operations get involved and is therefore much faster and more stable.

In the following part of the paper, we well first present the theories underlying our method in section 2. Then we give the algorithm pipeline and the implementation details of each step in section 3. The experimental results are reported in 4, followed by a conclusion and a brief discussion on the future direction in 5.

2 Theoretic Background

In this section, we briefly introduce the theoretic background necessary for understanding the algorithm proposed here.

Intuitively, a tangent vector field on a surface is *harmonic*, if both its circulation and divergence are zeros. Two harmonic fields form a *holomorphic one-form*, if they are orthogonal everywhere. An intrinsic way to compute conformal parameterization is to search for a *holomorphic one-form* that satisfies certain properties. In order to acquire the canonical mapping to the slit domains, we shall find certain holomorphic one-forms with special behavior on the boundary of the surface.

2.1 Harmonic Function

Suppose S is a surface embedded in $\mathbb{R}^3$ with induced Euclidean metric $\mathbf{g}$. S is covered by an atlas $\{(U_\alpha, \phi_\alpha)\}$. Suppose (x_α, y_α) is the local parameter on the chart (U_α, ϕ_α). We say (x_α, y_α) is *isothermal*, if the metric has the representation

$$\mathbf{g} = e^{2\lambda(x_\alpha, y_\alpha)}(dx_\alpha^2 + dy_\alpha^2).$$

The *Laplace-Beltrami operator* is defined as

$$\Delta_{\mathbf{g}} = \frac{1}{e^{2\lambda(x_\alpha, y_\alpha)}}(\frac{\partial^2}{\partial x_\alpha^2} + \frac{\partial^2}{\partial y_\alpha^2}).$$

Definition 1 (Harmonic Function). *A function $f : S \to \mathbb{R}$ is* harmonic*, if $\Delta_{\mathbf{g}} f \equiv 0$.*

2.2 Holomorphic One-form

Suppose ω is a differential one-form with the representation $f_\alpha dx_\alpha + g_\alpha dy_\alpha$ in the local parameters (x_α, y_α), and $f_\beta dx_\beta + g_\beta dy_\beta$ in the local parameters (x_β, y_β). Then

$$\begin{pmatrix} \frac{\partial x_\alpha}{\partial x_\beta} & \frac{\partial y_\alpha}{\partial x_\beta} \\ \frac{\partial x_\alpha}{\partial y_\beta} & \frac{\partial y_\alpha}{\partial y_\beta} \end{pmatrix} \begin{pmatrix} f_\alpha \\ g_\alpha \end{pmatrix} = \begin{pmatrix} f_\beta \\ g_\beta \end{pmatrix}.$$

ω is a *closed one-form*, if on each chart (x_α, y_α)

$$\frac{\partial f}{\partial y_\alpha} - \frac{\partial g}{\partial x_\alpha} = 0.$$

ω is an *exact one-form*, if it equals the gradient of some function. An exact one-form is also a closed one-form. If a closed one-form ω satisfies

$$\frac{\partial f}{\partial x_\alpha} + \frac{\partial g}{\partial y_\alpha} = 0,$$

then ω is a *harmonic one-form*. The gradient of a harmonic function is an exact harmonic one-form.

The so-called *Hodge star operator* turns a one-form ω to its *conjugate* ${}^*\omega$,

$${}^*\omega = -g_\alpha dx_\alpha + f_\alpha dy_\alpha.$$

Definition 2 (Holomorphic One-form). *A holomorphic one-form is a complex differential form*

$$\omega + \sqrt{-1}^{*}\omega,$$

where ω is a harmonic one-form.

The wedge product of two one-forms $\omega_k = f_k dx + g_k dy, k = 1, 2$ is a two-form

$$\omega_1 \wedge \omega_2 = (f_1 g_2 - f_2 g_1) dx \wedge dy.$$

2.3 Slit Mapping

Suppose S is an open surface with n boundaries $\gamma_1, \cdots, \gamma_n$. We can uniquely find a holomorphic one-form ω, such that

$$\int_{\gamma_k} \omega = \begin{cases} 2\pi & k = 1 \\ -2\pi & k = 2 \\ 0 & otherwise \end{cases}$$

Definition 3 (Circular Slit Mapping). *Fix a point p_0 on the surface, for any point $p \in S$, let γ be an arbitrary path connection p_0 and p, then the circular slit mapping is defined as*

$$\phi(p) = e^{\int_\gamma \omega}.$$

The proof of the following theorem on slit mapping can be found in [24].

Theorem 1 (Canonical Domains for Multiply Connected Surface). *The function ϕ effects a one-to-one conformal mapping of M onto the annulus $1 < |z| < e^{\lambda_0}$ minus $n-2$ concentric arcs situated on the circles $|z| = e^{\lambda_i}, i = 1, 2, \cdots, n-2$.*

For a given choice of the inner and outer circle, the circular slit mapping is uniquely determined up to a rotation around the center.

The slit mapping computes the intrinsic structure of the given surface, which can be reflected in the shape of the target domain. The shape of a canonical region with connectivity n depends on $3n-6$ real constants. If we put the center of boundary circles at the origin, and chose the radius of the outre circle to be 1 by normalization, then the position and length of each concentric slit is determined by 3 numbers, which gives a total of $3n-6$; the radius of the inner circle requires an additional parameter, but another parameter must be discounted to allow for arbitrary rotation of the domain. Actually, $3n-6$ is exactly the dimension of the conformal equivalence class space for an annulus with n boundaries.

The parallel slit mapping can be defined in a similar way.

Definition 4 (Parallel Slit Mapping). *Let $\bar{S}$ be the universal covering space of the surface S, $\pi : \bar{S} \to S$ be the projection and $\bar{\omega} = \pi^{*}\omega$ be the pull back of ω. Fix a point $\bar{p}_0$ on $\bar{S}$, for any point $p \in \bar{S}$, let $\bar{\gamma}$ be an arbitrary path connection $\bar{p}_0$ and $\bar{p}$, then the parallel slit mapping is defined as*

$$\bar{\phi}(\bar{p}) = \int_{\bar{\gamma}} \bar{\omega}.$$

2.4 Discrete Approximation

All the concepts defined in the smooth setting can be approximated in the discrete setting. A smooth surface is approximated by a piecewise linear triangular mesh M. v_i represents a vertex, $[v_i, v_k]$ means a half-edge, $[v_i, v_j, v_k]$ is an oriented face.

A discrete zero-form is a function defined on the vertices $f : V \to \mathbb{R}$. A discrete one-form is a function defined on the edges $\omega : E \to \mathbb{R}$. A discrete two-form is a function defined on the faces. The boundary operator ∂ gives the boundary of an oriented edge and an oriented face.

$$\partial[v_i, v_j] = v_j - vi,$$

$$\partial[v_i, v_j, v_k] = [v_i, v_j] + [v_j, v_k] + [v_k, v_i].$$

The discrete exterior differential operator d is defined as the following. Suppose f is a zero-form, then df is a one-form:

$$df([v_i, v_j]) = f \circ \partial[v_i, v_j] = f(v_j) - f(v_i).$$

If ω is a one-form, then $d\omega$ is a two-form:

$$d\omega([v_i, v_j, v_k]) = \omega \circ \partial[v_i, v_j, v_k] = \omega[v_i, v_j] + \omega[v_j, v_k] + \omega[v_k, v_i].$$

Given a discrete one-form ω, if $d\omega$ is zero, the ω is closed. If there is a zero-form f, such that $\omega = df$, then ω is exact.

Suppose ω is a closed one-form, then we can embed each face on the plane and assign it with a local coordinates. The discrete one-form can be represented as a smooth one-form on the face. The Hodge star operator and the wedge product operator can be defined the same as in smooth case.

The Laplace-Beltrami operator can be approximated by the cotangent formulae. A thorough discussion on the discrete Laplace-Beltrami operator can be found in Xu's work [19].

3 Algorithm Pipeline

In this work, our goal is to compute a conformal mapping from a multiply connected mesh to the slit domain. Suppose the input mesh has $n+1$ boundaries,

$$\partial M = \gamma_0 - \gamma_1 - \cdots - \gamma_n.$$

Without loss of generality, we map γ_0 to the outer circle of the circular slit domain, γ_1 to the inner circle, and all the others to the concentric slits.

The following is the algorithm pipeline:

1. Compute the basis for all exact harmonic one-forms; (*section 3.1*)
2. Compute the basis for all closed harmonic one-forms; (*section 3.2*)
3. Compute the basis for all holomorphic one-forms; (*section 3.3*)
4. Construct the slit mapping. (*section* **??**).

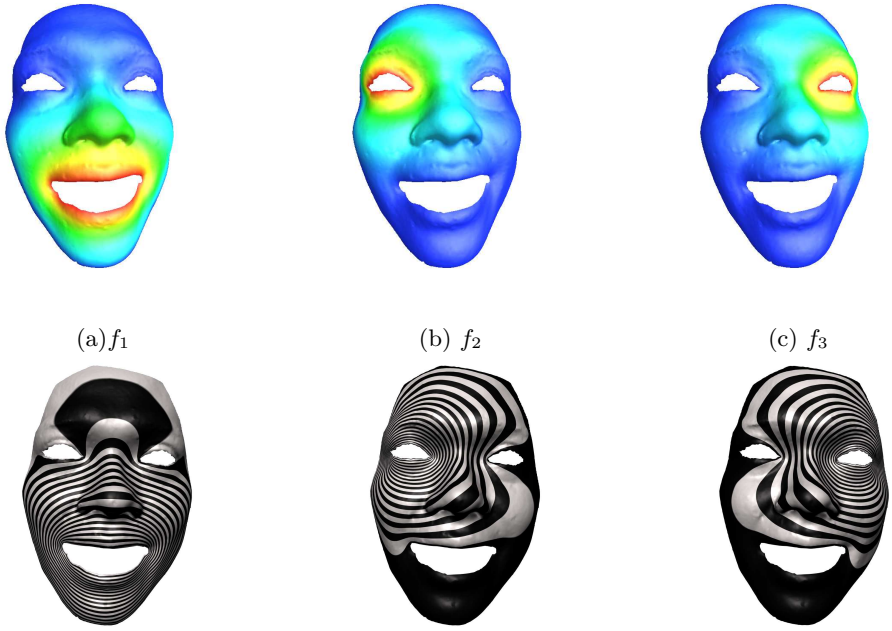

(a)f_1 (b) f_2 (c) f_3

(d)η_1 (e) η_2 (f) η_3

Fig. 3. Harmonic functions for three different inner boundaries. The first row shows the harmonic function f_k by color-encoding, the second row shows the corresponding harmonic one-form η_k by integration contours.

3.1 Basis of Exact Harmonic One-form

The first step of the algorithm is to compute the basis for exact harmonic one-forms. Let γ_k be an inner boundary, we compute a harmonic function $f_k : S \to \mathbb{R}$ by solving the following Dirichlet problem on mesh M:

$$\begin{cases} \Delta f_k \equiv 0 \\ f_k|_{\gamma_j} = \delta_{kj} \end{cases}$$

where δ_{kj} is the Kronecker function, Δ is the discrete Laplacian-Beltrami operator using the well-known co-tangent formula proposed in [16].

The exact harmonic one-form η_k can be computed as the gradient of the harmonic function f_k,

$$\eta_k = df_k,$$

and $\{\eta_1, \eta_2, \cdots, \eta_n\}$ form the basis for the exact harmonic one-forms .

3.2 Basis for Harmonic One-forms

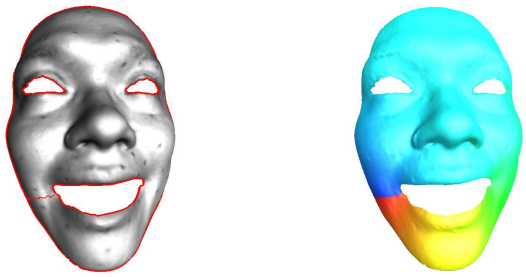

(a) ζ_1 (b) g_1

Fig. 4. Constructing a closed one-form. (a) shows the cut path ζ_1 on M bridging the inner boundary γ_1 to the outer boundary γ_0; (b) shows the harmonic function g_1 on the cut mesh M_1.

After getting the exact harmonic one-forms, we will compute the closed one-form basis. Let γ_k $(k > 0)$ be an inner boundary. Compute a path from γ_k to γ_0, denote it as ζ_k as shown in figure 4. ζ_k cut the mesh open to M_k, while ζ_k itself is split into two boundary segments ζ_k^+ and ζ_k^- in M_k. Define a function $g_k : M_k \to \mathbb{R}$ by solving a Dirichlet problem,

$$\begin{cases} \Delta g_k \equiv 0 \\ g_k|_{\zeta_k^+} = 1 \\ g_k|_{\zeta_k^-} = 0. \end{cases}$$

(a)τ_1 (b)τ_1 (c)τ_3

Fig. 5. Basis for the closed but not exact harmonic one-forms.

Compute the gradient of g_k and let $\tau_k = dg_k$, then map τ_k back to M, where τ_k becomes a closed one-form. Then we need to find a function $h_k : M \to \mathbb{R}$, by solving the following linear system:

$$\Delta(\tau_k + dh_k) \equiv 0.$$

Updating τ_k to $\tau_k + dh_k$, now we have $\{\tau_1, \tau_2, \ldots, \tau_n\}$ as a set of basis for all the closed but not exact harmonic one-forms. Figure 5 shows the closed non-exact harmonic one-form basis for the face model.

With both the exact harmonic one-form basis and the closed non-exact harmonic one-form basis computed, we can construct the harmonic one-form basis by taking the union of them:

$$\{\eta_1, \eta_2, \cdots, \eta_n, \tau_1, \tau_2, \cdots, \tau_n\}.$$

3.3 Basis for Holomorphic One-forms

$(\eta_1 + {}^*\eta_1)$ $(\eta_2 + {}^*\eta_2)$ $(\eta_3 + {}^*\eta_3)$

Fig. 6. Holomorphic one-form basis.

In step 1 we computed the basis for exact harmonic one-forms $\{\eta_1, \cdots, \eta_n\}$. Now we compute their conjugate one-forms $\{{}^*\eta_1, \cdots, {}^*\eta_n\}$, so that we can combine all of them together into a set of holomorphic one-form basis.

First of all, for η_k we compute an initial approximation η_k' by a brute-force method using Hodge star. That is, rotating η_k by 90° about the surface normal to obtain η_k'. In practice such an initial approximation is usually not accurate enough. In order to improve the accuracy, we employ a technique utilizing the harmonic one-form basis we just computed. From the fact the η_k is harmonic, we can conclude that its conjugate ${}^*\eta_k$ should also be harmonic. Therefore, ${}^*\eta_k$ can be represented as a linear combination of the base harmonic one-forms:

$$ {}^*\eta_k = \sum_{i=1}^{n} a_i \eta_i + \sum_{i=1}^{n} b_i \tau_i. $$

Using the wedge product $\wedge$, we can construct the following linear system,

$$ \int_M {}^*\eta_k \wedge \eta_i = \int_M \eta_k' \wedge \eta_i, \int_M {}^*\eta_k \wedge \tau_j = \int_M \eta_k' \wedge \tau_j. $$

We solve this linear system to obtain the coefficients a_i and b_i $(i = 1, 2, \cdots, n)$ for the conjugate one-form ${}^*\eta_k$. Pairing each base exact harmonic one-form with its conjugate, we get a set of basis for the holomorphic one-form group on M:

$$ \{\eta_1 + \sqrt{-1}{}^*\eta_1, \cdots, \eta_n + \sqrt{-1}{}^*\eta_n\} $$

Figure 6 demonstrates the base holomorphic one-forms on the mesh.

3.4 Construct Slit Mapping

After computing the holomorphic one-form basis, we need to find a special holomorphic one-form ω

$$ \omega = \sum_{i=1}^{n} \lambda_i (\eta_i + \sqrt{-1}{}^*\eta_i) $$

such that the imaginary part of its integration satisfies

$$ Im\left(\int_{\gamma_k} \omega\right) = \begin{cases} -2\pi & k = 1 \\ 0 & k > 1 \end{cases} $$

In order to get the coefficients λ_i, solve the following linear system for λ_i, $i = 1, \cdots, n$:

$$ \begin{pmatrix} \alpha_{11} & \alpha_{12} & \cdots & \alpha_{1n} \\ \alpha_{21} & \alpha_{22} & \cdots & \alpha_{2n} \\ \vdots & \vdots & \ddots & \vdots \\ \alpha_{n1} & \alpha_{n2} & \cdots & \alpha_{nn} \end{pmatrix} \begin{pmatrix} \lambda_1 \\ \lambda_2 \\ \vdots \\ \lambda_n \end{pmatrix} = \begin{pmatrix} -2\pi \\ 0 \\ \vdots \\ 0 \end{pmatrix} $$

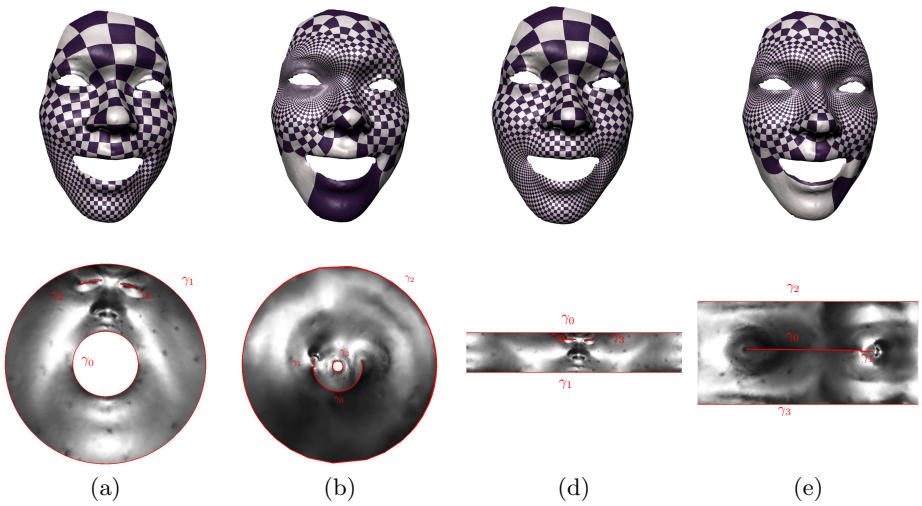

Fig. 7. Circular Slit Mapping and Parallel Slit Mapping. The first row shows the conformal texture mappings induced by the slit mappings; the second row shows the corresponding slit domains.

where

$$\alpha_{kj} = \int_{\gamma_j} {}^*\eta_k,$$

It can be proven that this linear system has a unique solution, which reflects the fact that γ_1 is mapped to the inner circle of the circular slit domain. Further, the system implies the following equation

$$\lambda_1\alpha_{01} + \lambda_2\alpha_{02} + \cdots + \lambda_n\alpha_{0n} = 2\pi,$$

which means that γ_0 is mapped to the outer circle in the circular slit domain.

After computing the desired holomorphic one-form ω, we are ready to generate the circular slit mapping. What we need to compute is a complex-valued function $\phi : M \to \mathbb{C}$ by integrating ω and taking the exponential map. Choosing a base vertex v_0 arbitrarily, and for each vertex $v \in M$ choosing the shortest path γ from v_0 to v, we can compute the map as the following:

$$\phi(v) = e^{\int_\gamma \omega}.$$

Based on the circular slit map ϕ we just computed, we can compute a parallel slit map $\tau : M \to \mathbb{C}$:

$$\tau(v) = \ln \phi(v).$$

Figure 7 shows the results for both circular and parallel slit mappings. In the third frame, γ_0 and γ_1 are mapped to the outer and inner boundaries, γ_2 and γ_3 to the circular slits. In the second frame, γ_2 and γ_3 are mapped to the outer and inner boundaries, γ_0 and γ_1 to the circular slits. Frame 3 shows the parallel slit

mapping, which is the logarithm of the circular slit mapping in the first frame; Frame 4 is the logarithm of the circular slit mapping in the second frame.

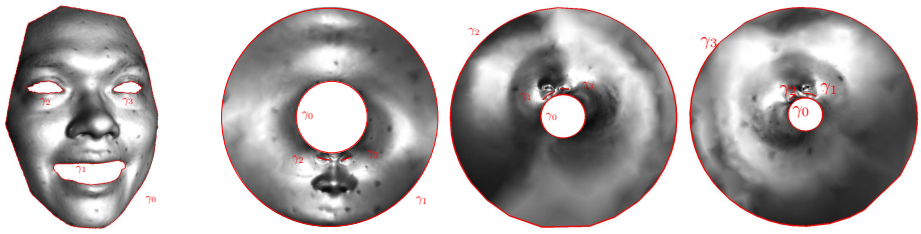

Fig. 8. Circular slit mappings with different boundary arrangements.

Figure 8 shows more circular slit mappings. Any two boundaries can be chosen and be mapped to the outer and inner circles.

4 Experimental Results

We implemented our algorithm in C++ on Windows platform. The system has been tested on several real human face surfaces (see figure 10), scanned by 3D scanners introduced in [**?**]. Each face mesh has around $15k$ vertices and $30k$ triangles with 4 boundaries. We also tested our system on a brain cortical surface (figure 11), which is reconstructed from MRI images. The cortical surface has $30k$ vertices and $60k$ faces with 12 landmarks sliced on the surface. The harmonic forms are computed using a brute-force implementation of the conjugate gradient method, without using any well-tuned numerical library. The whole processing takes less than 3 minuets. In all experiments the algorithm converges stably, and the final parameterization results are conformal.

As a global conformal parameterization method, slit mapping can be applied to many applications in geometric modeling and processing. In the current work we applied slit mapping method for several most direct applications and got some preliminary results.

Texture Mapping. One of most direct applications in computer graphics is texture mapping. As shown in figure 1, the parallel slit domain can serve as the texture domain, which is very regular in shape. More over, the texture domain is fully utilized during the texture mapping, since there is no gap inside the domain.

Although this work focuses on multiply connected surfaces, in fact our algorithm can be easily generalized to handle high genus closed surfaces, such as the eight model in figure 9. The only extra requirement is to slice the surface open along certain cycles, for example, the two tunnel cycles in figure 9c. Such cycles can be automatically computed using methods like that proposed by T. Dey et

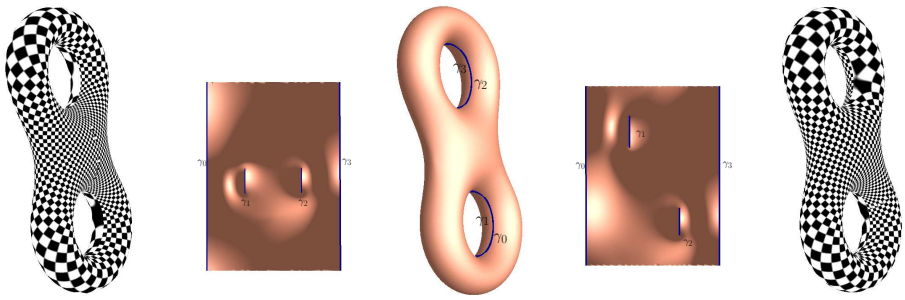

Fig. 9. Slit mapping of closed mesh. The closed eight model needs to be sliced open along two tunnel cycles and turned into an annulus with 4 boundaries, as shown in (c). (a) is the texture mapping using texture domain (b), which is the parallel slit domain with prescribed boundary γ_0 and γ_2; (e) is the texture mapping using texture domain (d), which is the parallel slit domain with prescribed boundary γ_0 and γ_3.

al in [17]. After turning the surface into a multiply connected one, we can carry out the slit algorithm thereafter directly.

Surface Fingerprint. The slit mapping method computes the conformal invariants of the surface. The shape parameters of the circular slit domain indicate the conformal equivalence class of the surface and can be treated as the fingerprints of the surface. We test our algorithm for several human faces from different persons with different expressions. The result is illustrated in figure 10. From this figure, it is very clear that the fingerprints of the three calm faces are very similar, whereas the fingerprint of the laughing face is quite different from others. This gives us a way to measure the expression quantitatively.

Conformal Brain Mapping with Landmarks. Slit mapping provides a valuable tool for brain mapping. As shown in figure 11, brain surfaces are highly convoluted. It is a great challenge to match two cortical surfaces directly in $\mathbb{R}^3$. Conformal brain mapping flattens the brain surface onto the canonical domains. Special landmarks are labeled on the surface, which are required to be registered across different brain surfaces. By using slit mapping, all the land marks are mapped to parallel slits, and the whole brain is mapped to a rectangle. This makes the down stream registration and analysis much easier. In the middle column of figure 11, the circular slit mapping result is illustrated. In order to show the landmarks clearly, we remove the texture information from the surface in the bottom frame. The last column shows the parallel slit mapping result; all the landmarks are mapped to horizontal slits as illustrated in the bottom frame.

As a general method for conformal parameterization, slit mapping can also benefits many other applications, such as quad-remeshing, geometry image generation, mesh-spline conversion and etc. It is an interesting research direction to explore the potential of our method in those applications.

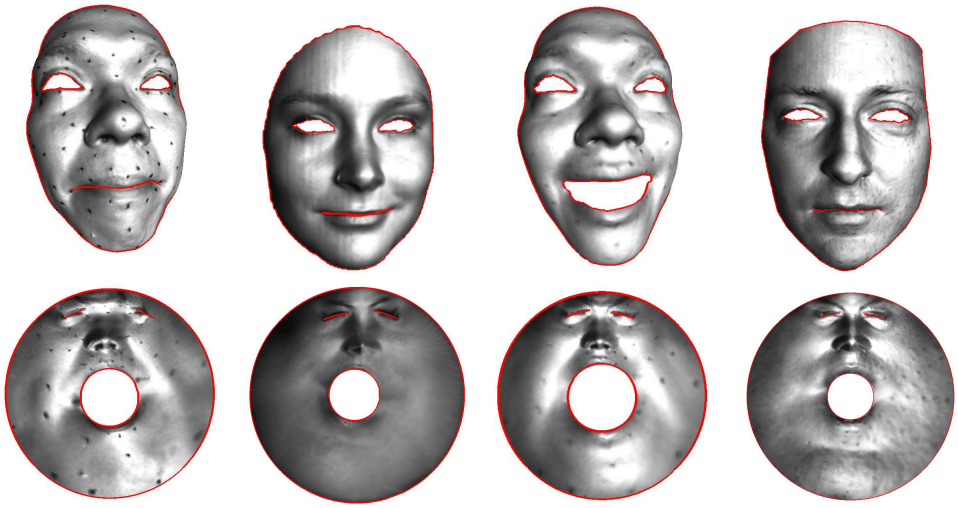

Fig. 10. Slit domains as finger prints. The left column shows two face models; the middle and right column show their finger prints using the parallel and circular slit domains respectively.

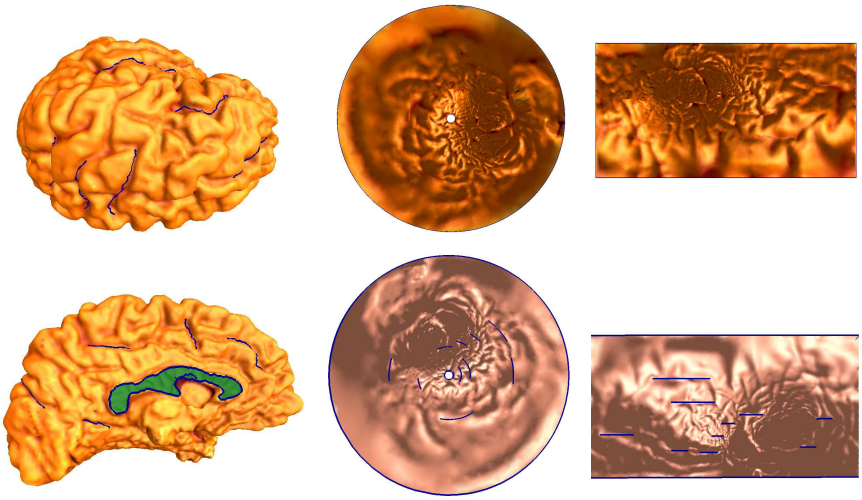

Fig. 11. Conformal brain mapping with 12 landmarks. The first column is the brain surface; the second column is the circular slit mapping; the last column is the parallel slit mapping.

5 Conclusion

In this work, we presented a novel global conformal parameterization method, called slit map, for multiply connected surfaces. The method is based on computing a holomorphic one-form that has special behaviors on the surface boundaries. The algorithm maps any multiply connected surface to a flat annulus with concentric circular slits (circular slit domain) or to a rectangle with parallel slits (parallel slit domain). The target domains are canonical and reflect the intrinsic conformal structure of the surface; therefore, the shape parameters of the target domains can be used for conformal surface classification. The method can benefit many important applications in geometric modeling and processing, such as texture mapping, surface classification, quad re-meshing, mesh-spline conversion and so on. It can also be applied for conformal brain mapping in medical imaging field. The regularity of the target domain facilitates surface matching with land mark constraints. The method is automatic, efficient, stable and general, which can be shown by our experimental results

In the future, we will explore more applications of slit mapping. Also, we want to investigate alternative methods of conformal mapping for multiply connected surfaces and compare their performances to that of slit mapping.

Acknowledgments We wish to thank Geometric Informatics Inc. for supplying the 3D face data sets. We also thank UCLA neurology department for supplying the cortex surface model. This work was partly supported by NSF.

References

1. SHEFFER, A., DE STURLER, E.: Parameterization of Faceted Surfaces for Meshing Using Angle Based Flattening. Engineering with Computers 17(3), pp. 326–337.
2. SHEFFER, A., PRAUN, E., ROSE, K.: Mesh Parameterization Methods and their Applications. Now Publishers, 2006, ISBN 978-1-933019-43-7.
3. FLOATER, M.: Mean value coordinates. CAGD, 20(1), 19–27.
4. FLOATER, M., HORMANN, K.: Surface Parameterization: a Tutorial and Survey. Advances in Multiresolution for Geometric Modelling, pp. 157–186.
5. ECK, M., DEROSE, T., DUCHAMP, T., HOPPE, H., LOUNSBERY, M., STUETZLE, W.: Multiresolution analysis of arbitrary meshes. ACM SIGGRAPH 95, pp. 173–182.
6. LÉVY, B., PETITJEAN, S., RAY, N., MAILLOT, J.: Least squares conformal maps for automatic texture atlas generation. ACM SIGGRAPH 2002, pp. 362–371.
7. DESBRUN, M., MEYER, M., ALLIEZ, P.: Intrinsic parameterizations of surface meshes. Computer Graphics Forum, 21 (2002), pp. 209–218.
8. KARNI, Z., GOTSMAN, C., GORTLER, S.: Free-boundary linear parameterization of 3D meshes in the presence of constraints. Proceedings of Shape Modeling and Applications 2005.
9. COHEN-STEINER, D., ALLIEZ, P., DESBRUN, M.: Variational shape approximation. ACM SIGGRAPH 2004, pp. 905–914.

10. GARLAND, M., WILLMOTT, A., HECKBERT, P.: Hierarchical Face Clustering on Polygonal Surfaces. Proceedings of ACM Symposium on Interactive 3D Graphics 2001.
11. MAILLOT, J., YAHIA, H., VERROUST, A.: Interactive texture mapping. ACM SIGGRAPH '93, pp. 27–34.
12. SANDER, P., WOOD, Z.,GORTLER, S., SNYDER, J., HOPPE, H.: Multi-chart geometry images. ACM Symposium on Geometry Processing 2003.
13. GU, X., YAU, S.-T.: Computing conformal structures of surfaces. Communications in Information and Systems, 2(2), pp. 121–146.
14. GU, X., YAU, S.-T.: Global conformal surface parameterization. Symposium on Geometry Processing 2003, 127–137.
15. JIN, M., KIM, J., GU, X.: Discrete surface ricci flow: Theory and applications. Lecture Notes in Computer Science, Vol.4647, pp.209–232. Springer, 2007.
16. PINKALL, U., POLTHIER, K.: Computing discrete minimal surfaces and their conjugates. Experim. Math. **2** (1993) 15–36
17. DEY, T. K., LI, K., SUN, J.: On computing handle and tunnel loops. IEEE Proc. NASAGEM 07 (to appear).
18. GORTLER, S.J., GOTSMAN, C., THURSTON, D.: Discrete One-Forms on Meshes and Applications to 3D Mesh Parameterization. Computer Aided Geometric Design, 33(2):83–112, 2006.
19. XU, G.: Discrete Laplace-Beltrami operators and their convergence. Computer Aided Geometric Design 2004: 767–784
20. TONG, Y., ALLIEZ, P., COHEN-STEINER, D., DESBRUN, M.: Designing quadrangulations with discrete harmonic forms. In Proc. Eurographics/ACM Symp. on Geom. Proc. (2006), pp. 201-C210.
21. KÄLBERER, F., NIESER, M., POLTHIER, K.: QuadCover - Surface Parameterization using Branched Coverings, Computer Graphics Forum, Eurographics 2007.
22. FISHER, M., SCHRÖDER, P., DESBRUN, M., HOPPE., H.: Design of tangent vector fields. ACM Transactions on Graphics (TOG) Vol 26, No 3, pp.56–66.
23. TONG, Y., LOMBEYDA, S., HIRANI, A. N., DESBRUN, M.: Discrete Multiscale Vector Field Decomposition. ACM Trans. Graph. 22, 3, pp.445–452.
24. AHLFORS, L.V.: Complex analysis. McGraw-Hill, New York, 1953.